Electronic Supplementary Material (ESI) for Environmental Science: Nano.

Supplemental Figures:

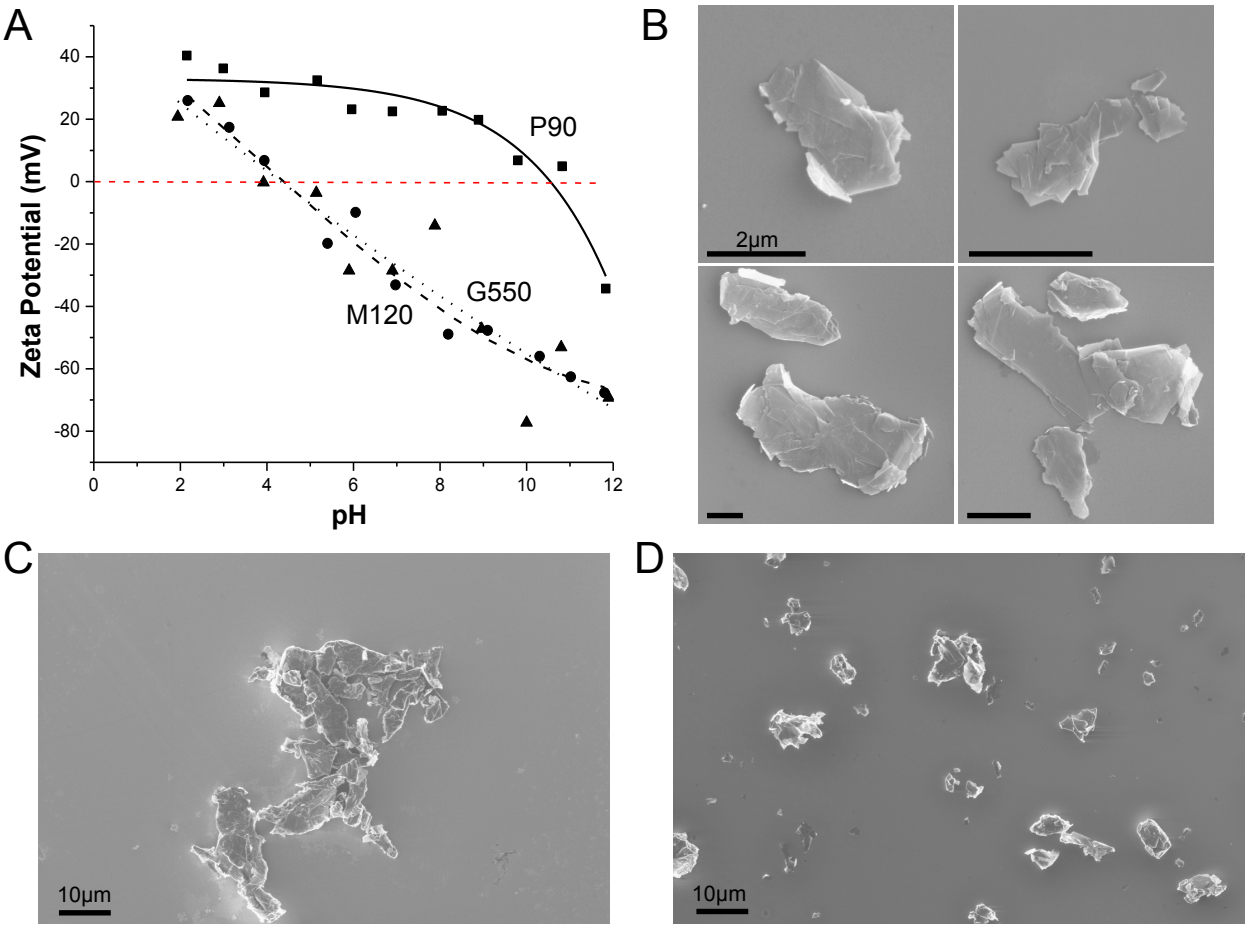

Figure S1. Additional nanomaterial characterization and adsorption data. A) Zeta potential was measured across a wide range of pH to determine the presence of charged groups on the carbon nanomaterials. At the biologically relevant pH 7, G550 and M120 have a similar negative potential, while P90 has a positive value, indicating differences in the type of functional groups on the two carbon black nanomaterials. B) Heterogeneity was observed in the size and shape of the G550 nanoplatelets. The G550 graphene microsheets were also re-examined by SEM after mixing for adsorption experiments (C) or dispersion through sonication prior to toxicity testing (D).

Table S1. Parameters and determination coefficients of Langmuir, Freundlich and Sips isotherm models. The equilibrium time is indicated in parenthesis.

	P90 (1 h)	P90 (12 h)	G550 (1 h)	G550 (12 h)	M120 (1 h)	M120 (12 h)
Langmuir						
Q_{max} ($mg \cdot g^{-1}$)	45.01	163.53	33.44	19.68	4.00	12.30
b ($L \cdot mg^{-1}$)	0.24	0.03	0.05	0.37	0.42	0.23
R_L	0.31	0.68	0.71	0.20	0.20	0.31
SSE[5]	0.54	1.77	1.21	1.17	0.10	0.21
R^2	0.997	0.994	0.972	0.992	0.991	0.995
Freundlich						
n	0.84	0.92	1.09	0.56	0.50	0.63
K_F	8.48	5.42	1.31	5.40	1.14	2.38
SSE	1.47	1.37	0.634	0.82	0.27	0.13
R^2	0.992	0.995	0.985	0.994	0.974	0.997
Sips						
b	0.60	0.05	0.10	0.29	0.44	0.11
Q_{max} ($mg \cdot g^{-1}$)	24.12	121.81	14.79	24.22	3.88	22.95
n	1.33	0.98	1.37	0.84	1.04	0.77
R_L	0.15	0.56	0.55	0.24	0.20	0.48
SSE	0.003	1.80	1.16	0.92	0.10	0.13
R^2	0.999	0.996	0.973	0.994	0.991	0.997

Table S2: Primer sequences gene expression analysis using RT-qPCR. Primers designed as described previously (Rodd et al. 2017).

Gene	Primer Sequence	GeneBank Accession No.	RT-qPCR Conditions
cyp1a	5': cgtcgctatgaccaccatga 3': atgaagtctgcagggttgcc	JX270831	0.2 µM primer in 2.5 mM $MgCl_2$
abcc2	5': gctggtcaccaccctctaca 3': ctggacttgtcctgagtgaagg	HM102360.1	0.4 µM primer in 3.0 mM $MgCl_2$
18S	5': tcggggaggtagtgacgaaa 3': caccagacttgccctccaat	HM102359	0.2 µM primer in 3.0 mM $MgCl_2$

Table S3: Characterization of functional groups on the carbon nanomaterials using acid-base titration.

	Acid-Base Functional Groups (meq/g)				
Samples	**Carboxylic**	**Lactonic**	**Phenolic**	**Carbonyl**	**Total**
P90	0.96	1.22	0.0	0.69	2.87
M120	1.175	0.465	0.18	0.706	2.52
G550	0.0	0.62	0.0	0.32	0.94

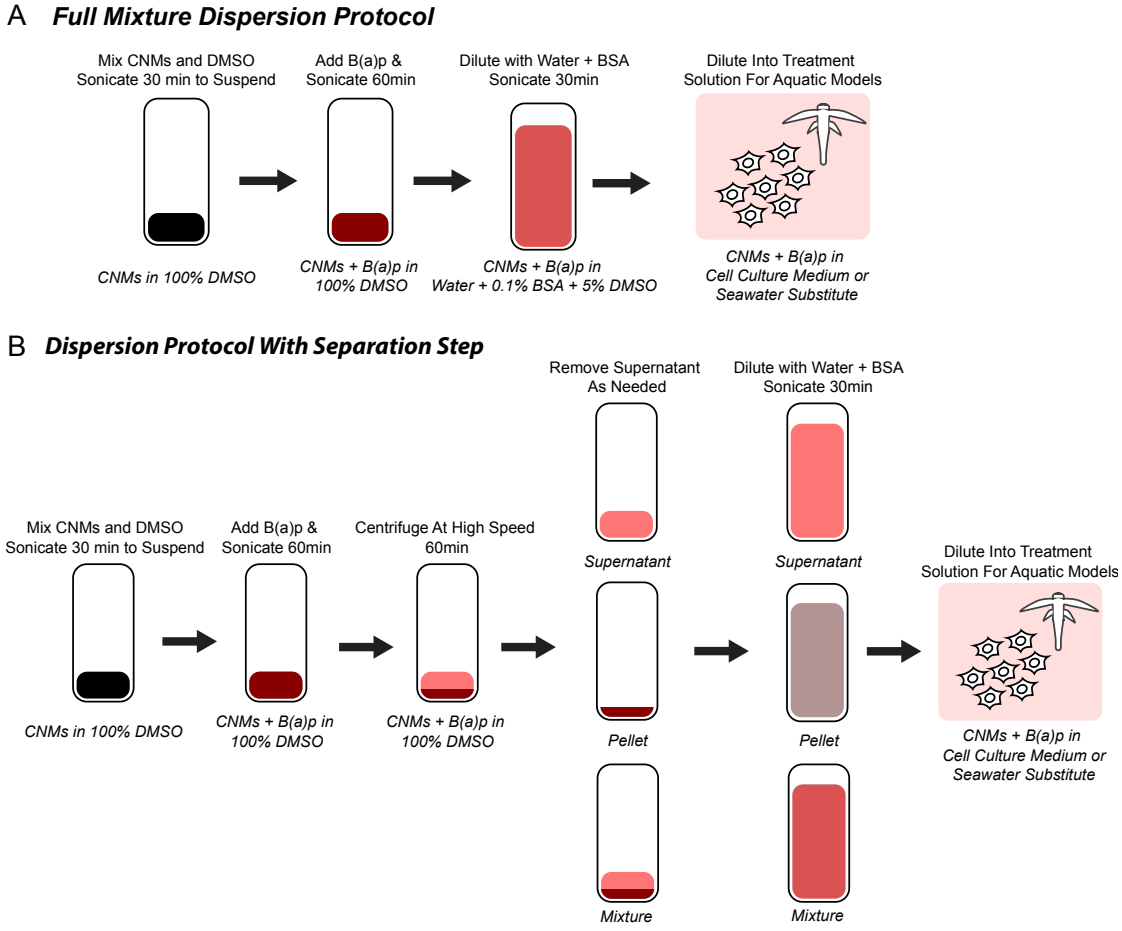

Figure S2. To more effectively deliver carbon nanomaterials to the biological model organisms, the dispersion protocol was modified to more evenly suspend the nanomaterials. A) For exposure to the full mixture, the carbon nanomaterials were first sonicated with benzo(a)pyrene in dimethyl sulfoxide (DMSO), then diluted with water and bovine serum albumin (BSA) and sonicated again. This stock solution was then diluted into exposure media at the final concentration for the experiment. B) For experiments using the fractionated mixture, after sonicating in DMSO the mixture was centrifuged at room temperature to separate out the pelleted fraction from the supernatant. For experiments with comparison to a full mixtures, the pellet and supernatant were left together after centrifugation. The different preparations were then diluted with water and BSA, sonicated, and diluted for toxicity testing.

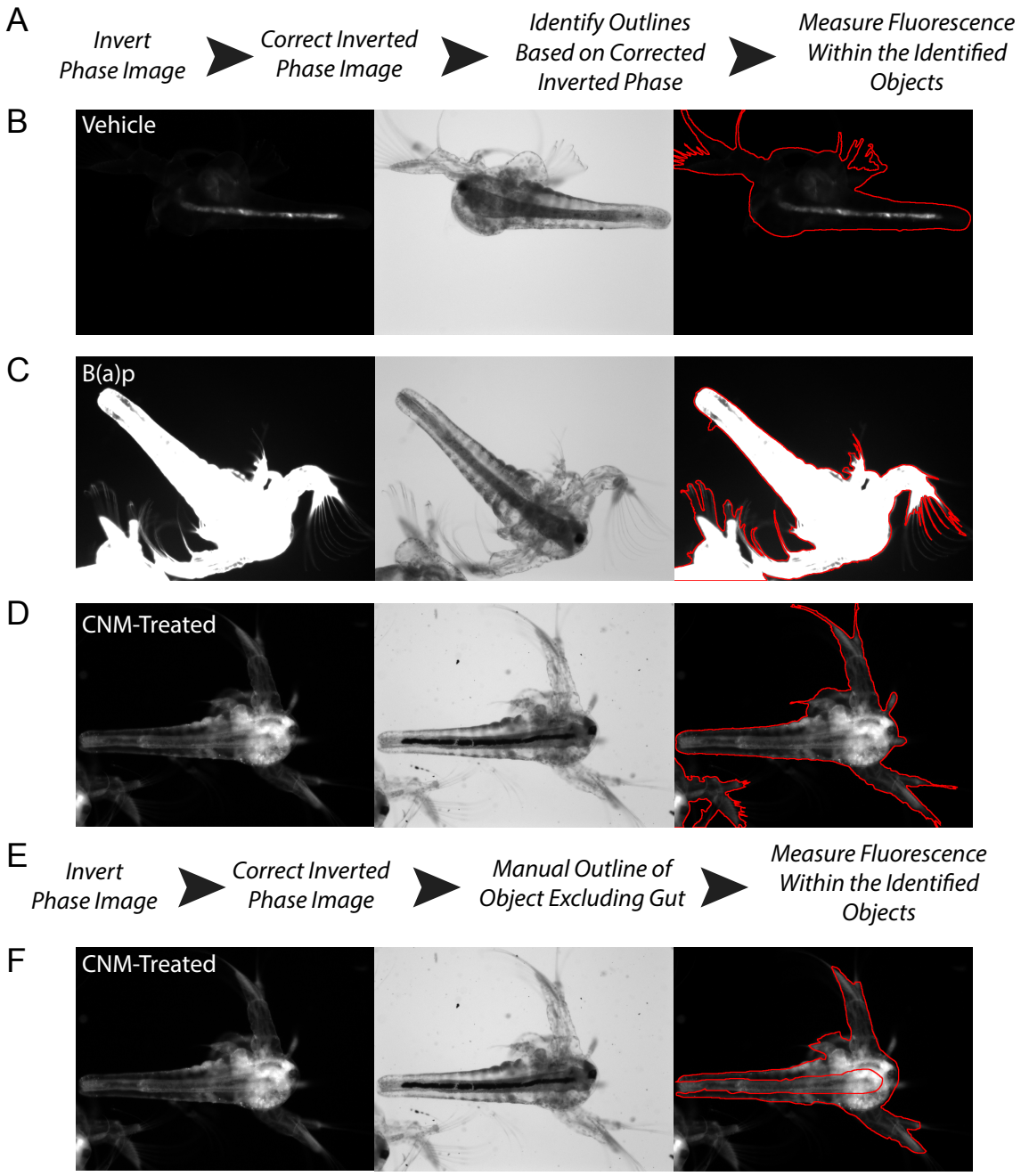

Figure S3. Brine shrimp image analysis. A) To analyze the fluorescence intensity of brine shrimp, a CellProfiler pipeline was created that used phase imaging to identify the brine shrimp (shown as a red outline in the images) and then measured the blue fluorescence intensity within that space. This method proved effective for all treatments, including vehicle-treated (B), benzo(a)pyrene-treated (C), and carbon nanomaterial-treated larvae (D). E) To conduct analysis with the gut excluded, brine needed to be manually identified. This selectively quantified fluorescence in the brine shrimp for comparative analysis (F).

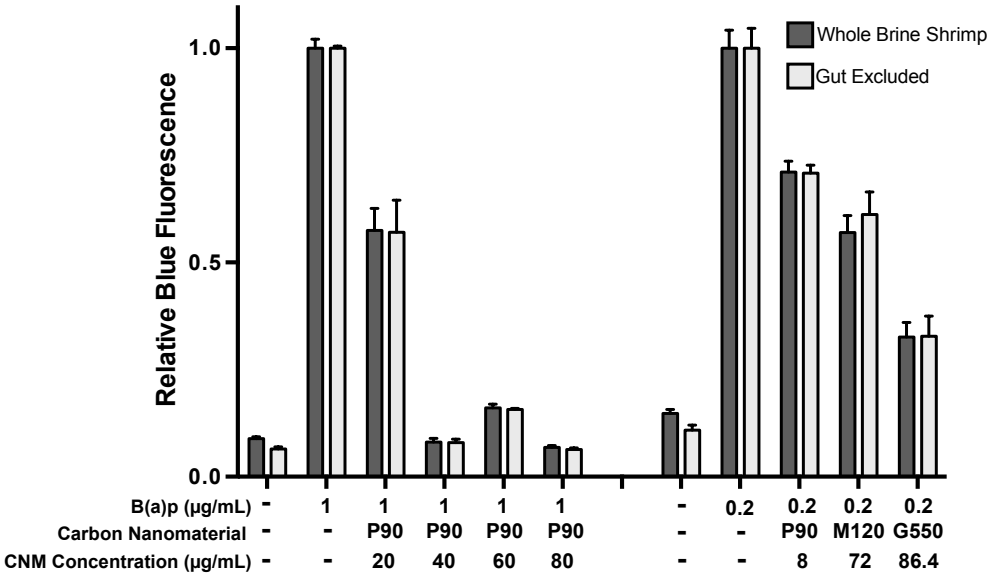

Figure S4. The same brine shrimp samples were analyzed with and without the gut contents to determine if the nanomaterials in the gut significantly altered the results. As shown above, no difference was observed between the two analysis techniques, allowing the whole brine shrimp technique to be used for subsequent analysis.

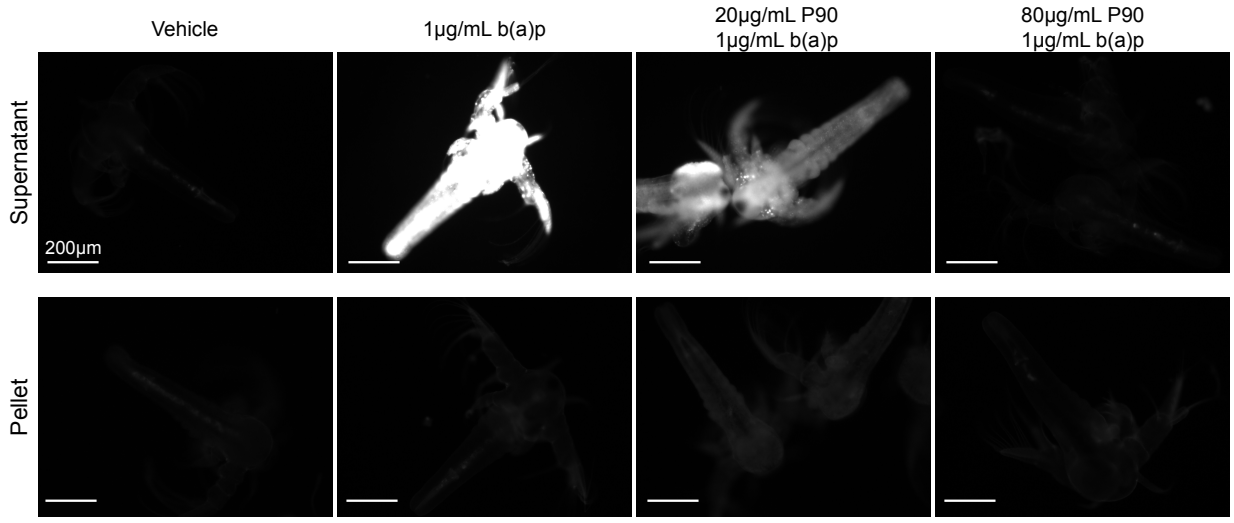

Figure S5. Brine shrimp fluorescence with separated P90 mixtures. Mixtures of P90 carbon and benzo(a)pyrene where mixed then separated into a supernatant or pelleted fraction for brine shrimp exposure. While the supernatant fraction shows significant fluorescence for the control and low P90 dose exposures, no significant fluorescence was observed in the pelleted exposures.

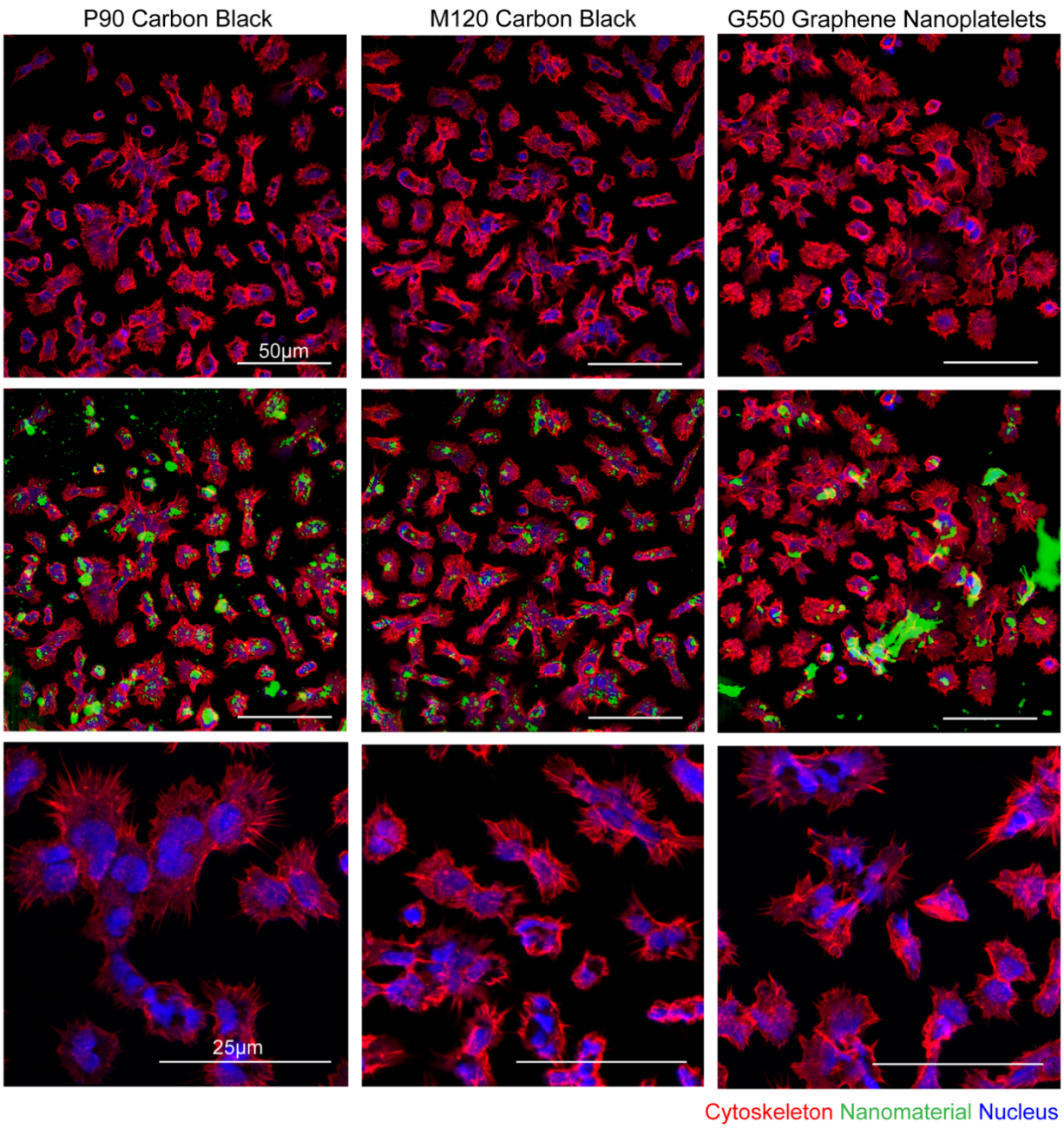

Figure S6. Cell morphology and nanomaterial uptake in PLHC-1 fish liver cells. Cells were treated with carbon nanomaterials (normalized by plating area to 30μg/mL) for 24hr, then processed for staining of the F-actin cytoskeleton with rhodamine phalloidin. Cell density was comparable across treatment groups, with no observable increase in cell loss. Carbon black nanomaterials appear readily phagocytosed by the cells, while only small G550 nanoplatelets were internalized. Bottom panel shows the cells at a higher magnification, with no change in cytoskeletal or nuclear morphology observed after nanomaterial treatment.

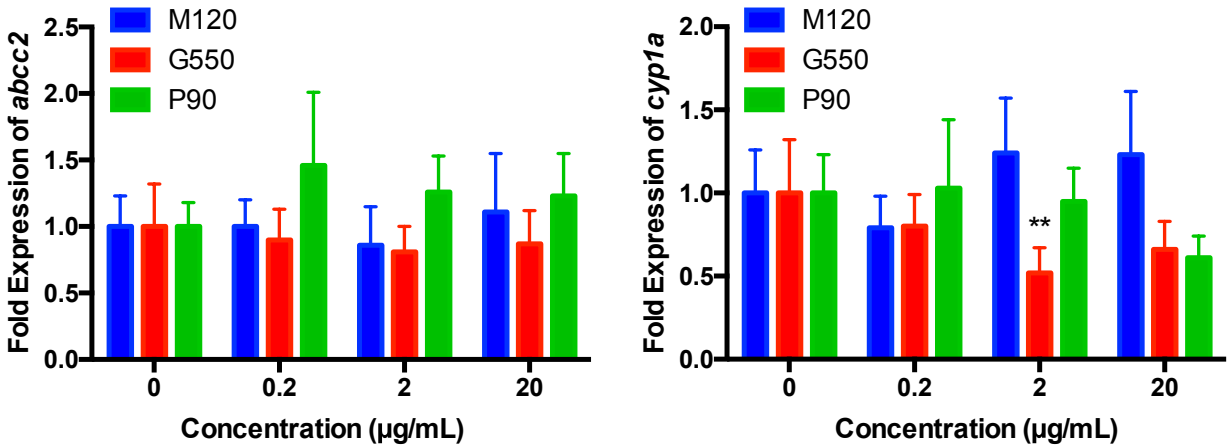

Figure S7. Gene expression response to 24hr nanomaterial exposure in PLHC-1 fish liver cells. While trends were observed, no statistically significant change in *abcc2* expression was measured in response to any of the three carbon nanomaterials. While G550 graphene microsheets caused significant downregulation of *cyp1a* after 24hr, both P90 carbon black and G550 graphene microsheets caused a downward trend in expression at 20µg/mL. In all cases, no change was great than +/- 2-fold over vehicle-treated cells. * $p < 0.05$; ** $p < 0.01$; *** $p < 0.001$.

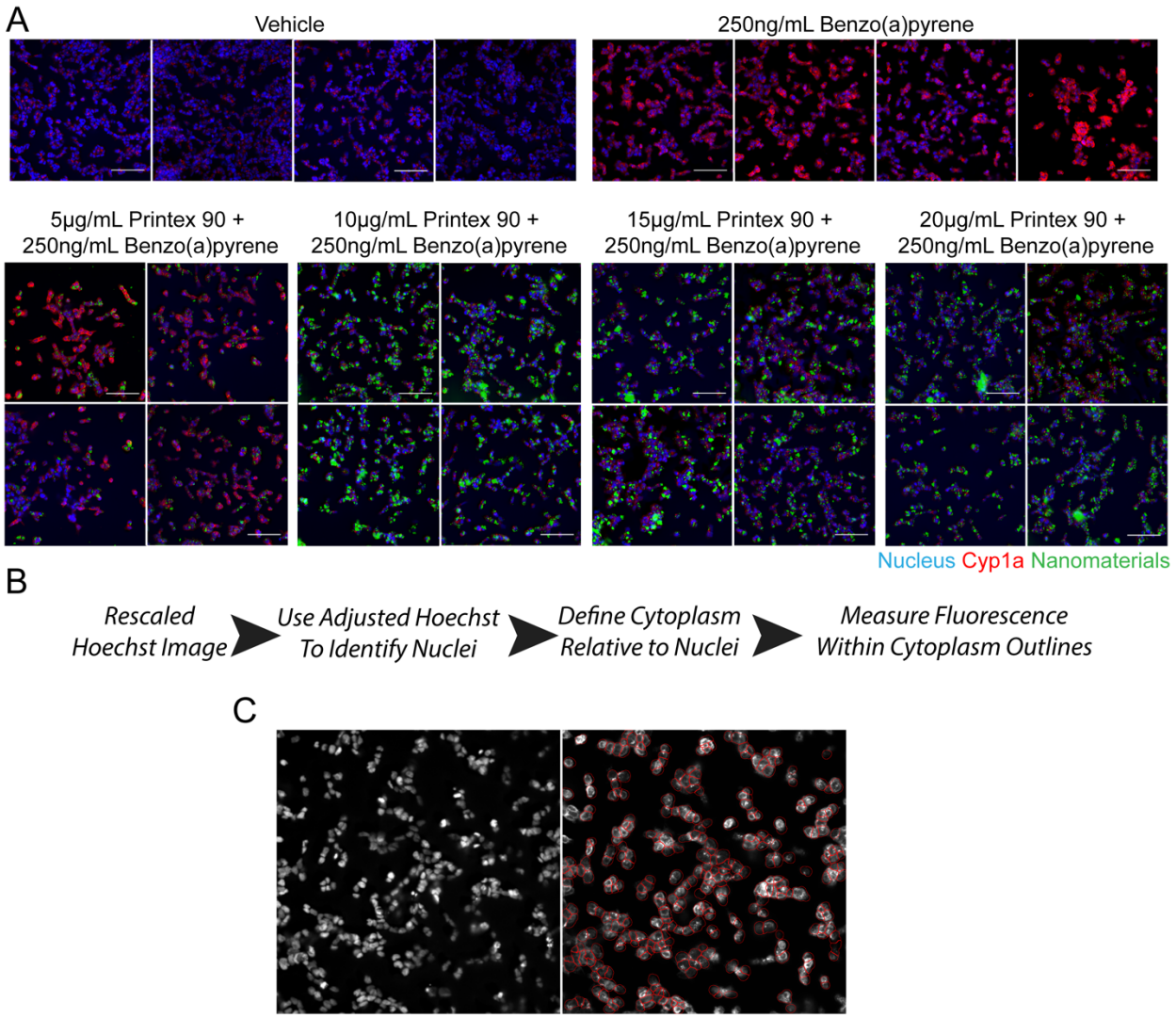

Figure S8. Image analysis of Cyp1a protein expression in PLHC-1 fish liver cells. To quantify relative levels of Cyp1a protein induced by these mixtures, four fields of view were imaged within each sample (A) and analyzed using a CellProfiler pipeline (B). Using the nuclear label, fluorescent Hoechst 33342 dye, the cytoplasm of the cell was defined as an area around the nucleus. Cyp1a immunofluorescence intensity was then measured within this defined area. C) An example of cell outlines is shown in the bottom panel, with the outline of the cytoplasm area shown in red.

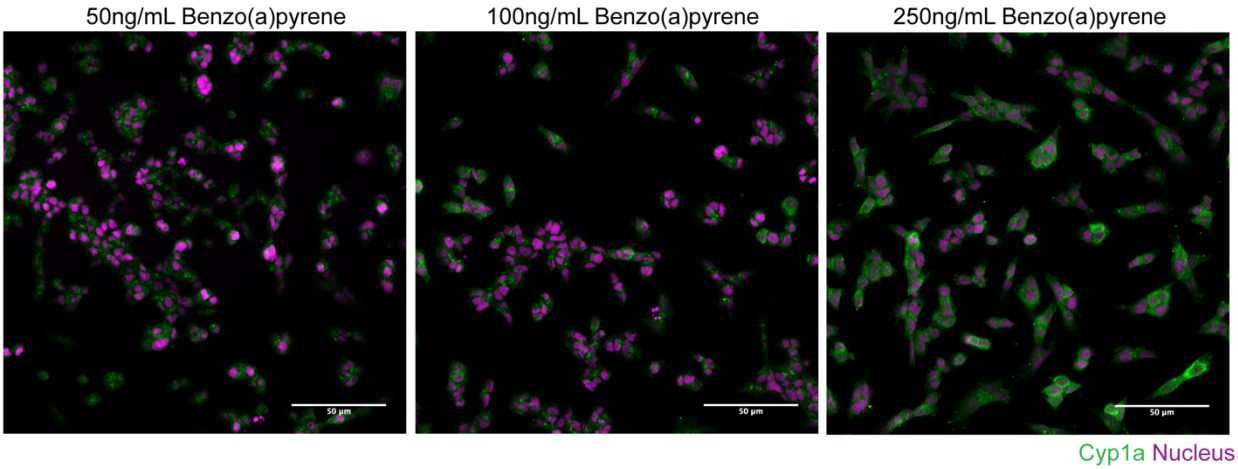

Figure S9. Induction of Cyp1a protein in response to benzo(a)pyrene. After 24 hr exposure to 50, 100 or 250ng/mL benzo(a)pyrene, fish liver cells were processed for immunofluorescence labeling of Cyp1a protein to demonstrate the sensitivity of the assay. After exposure 250ng/mL, most of the cells show increased fluorescence intensity with this technique. At 100ng/mL, only a small number of cells show increased fluorescence intensity, and at 50ng/mL no significant increase can be detected. In contrast, the highly sensitive quantification of *cyp1a* gene expression by qRT-PCR can detect >100-fold induction of *cyp1a* at 50ng/mL benzo(a)pyrene.

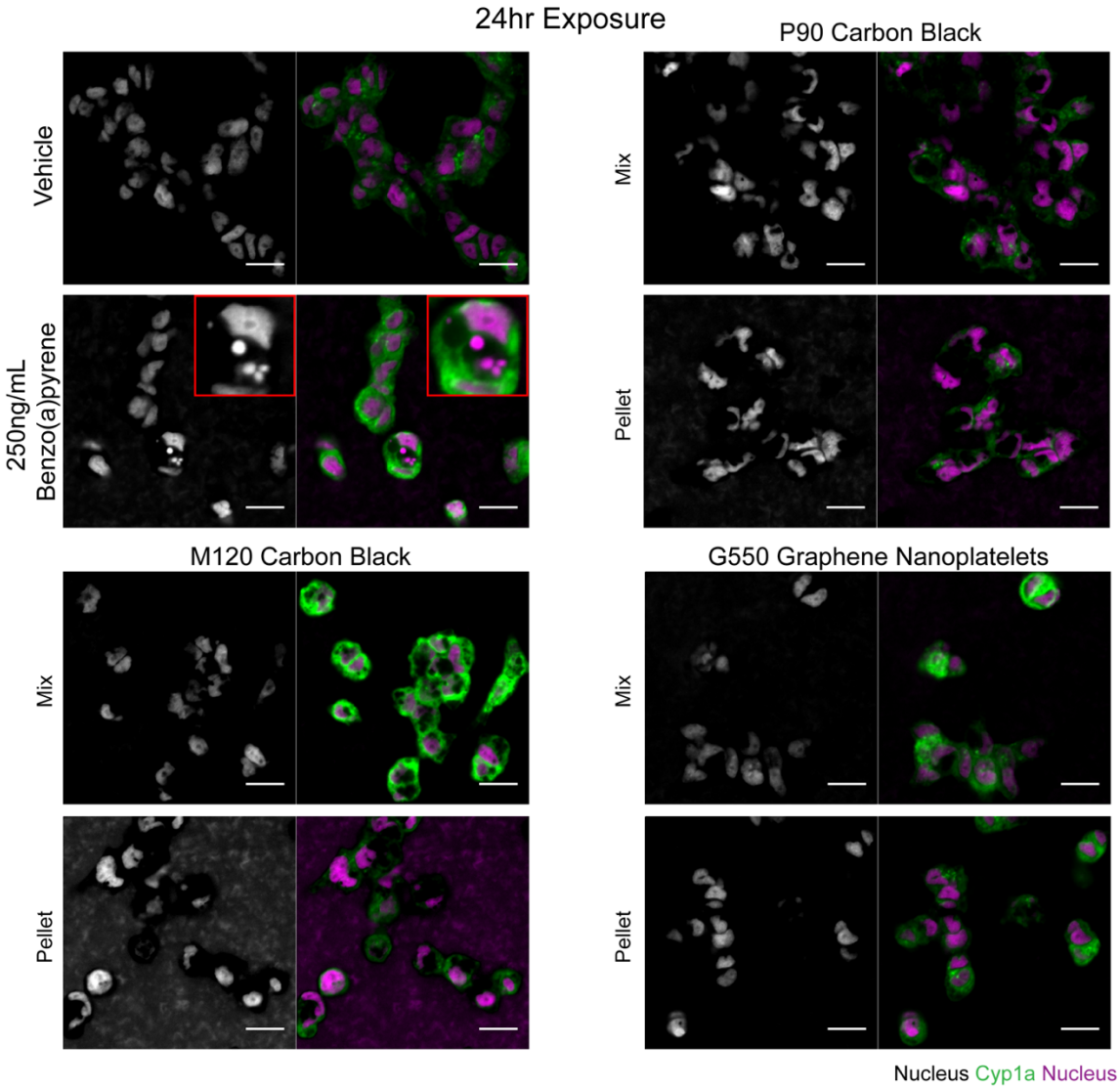

Figure S10. Highlighted nuclear morphology of cells after exposure to benzo(a)pyrene and carbon nanomaterials for 24hr. At the concentrations tested, few apoptotic nuclei were observed in any of the treatment groups. As an example, a cell with apoptotic nuclei observed in cells treated with 250ng/mL benzo(a)pyrene is highlighted in the red box as an inset.

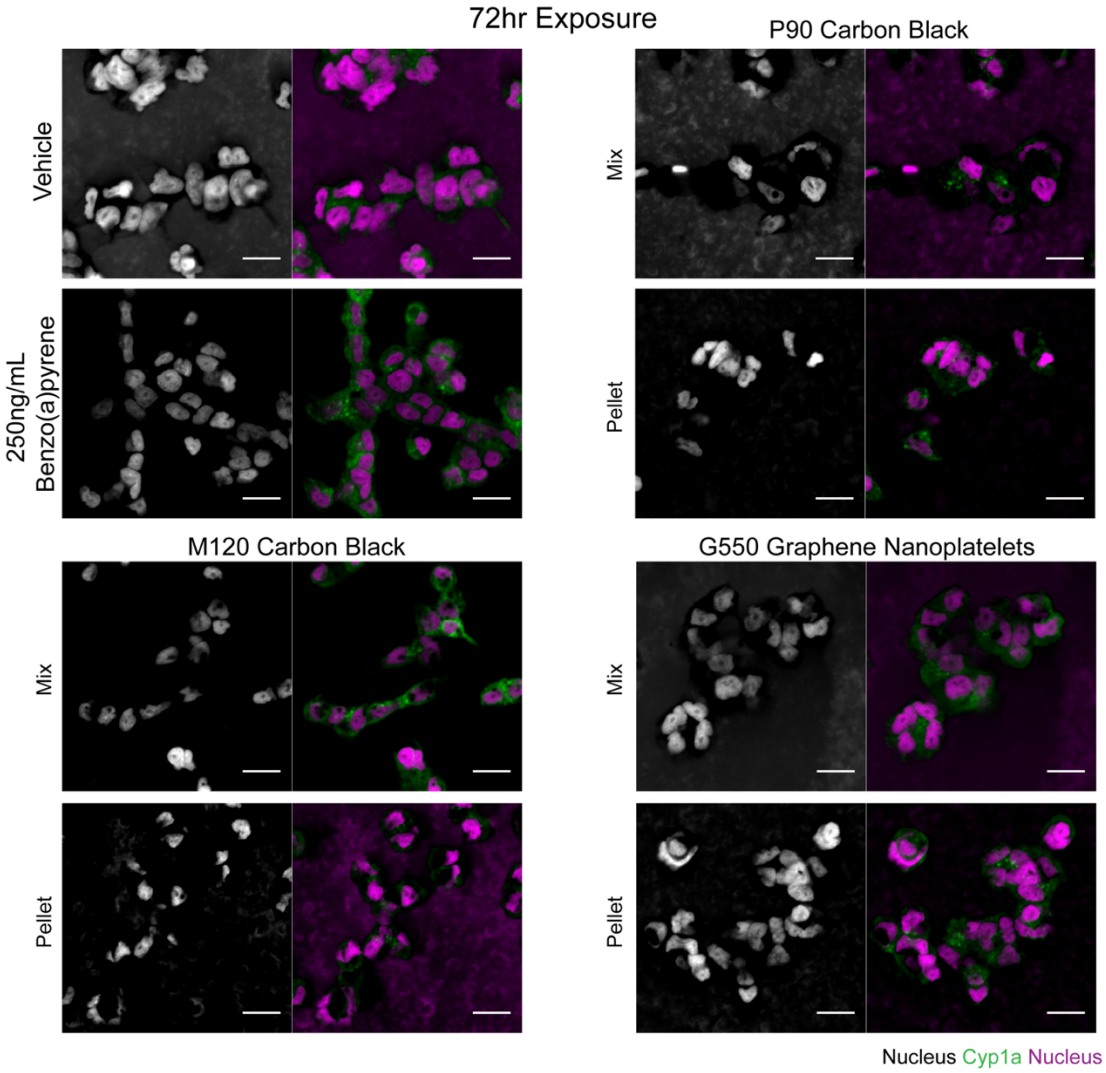

Figure S11. Highlighted nuclear morphology of cells after exposure to benzo(a)pyrene and carbon nanomaterials for 72hr. As observed after 24hr exposure, no differences in nuclear morphology were observed between the treatment groups.

APPENDIX 1. Computations for surface coverage by benzo[a]pyrene onto carbon-based materials

- CS (cross section area of BaP) = 255.6 $Å^2$ (Reference)
- BaP molecular weight = 264.3 g/mol
- N_A (Avogadro's number) = 6.022×10^{23}
- *m* (Mass of adsorbate= = 0.0075 g

Surface area of the carbon-based materials under study

- CB Printex 90 = 215.2
- FLG G550 = 33.2
- M120 = 32.8

A) Theoretical computations

Step 1) Computing m^2/mol BaP

$$CS \times N_A \times \frac{(1 \times 10^{-10})^2\ m^2}{1\ Å^2} = 1.54 \times 10^6\ m^2/\text{mol BaP}$$

Step 2) Computing mol BaP / m^2

If

$$1\ \text{mol BaP} \text{ ---------- } 1.54 \times 10^6\ m^2$$
$$X \text{ ---------- } 1\ m^2$$

$$X = 6.49 \times 10^{-7}\ \text{mol BaP}/m^2$$

Step 3) Computing the number of moles of BaP locateds in a specific surface area (S_{BET}) for the different adsorbents. Calculations are based on 1 g of the materials.
Example for CB Printex 90 (215 m^2/g):

$$6.5 \times 10^{-7}\ \text{mol BaP}/m^2 \times 215\ m^2/g = 1.3 \times 10^{-4}\ \text{mol BaP}/S_{BET}$$

*Step 4)*Computing mg BAP/S_{BET}, based in the mass of the adsorbate in the isotherm (0.0075 g).

$$1.3 \times 10^{-4}\ \text{mol BaP}/S_{BET} \times 264.3\ \text{g/mol} \times 1000\ \text{mg} \times |0.0075\ \text{g} = 0.277\ \text{mgBaP}/\ S_{BET} \cdot 7.5\ \text{mg}\ *$$

* This value represents the theoretical surface coverage of BaP by 7.5 mg of CB Printex 90

B) Experimental computations

*Step 5)*The first step is to take the values of the fitted adsorption isotherm based on a equilibrium concentration (C_e) of 6 mg/L. This example is based on the CB Printex 90 nanomaterial at 12 h.

q_e (Removal capacity) = 26.14 mg/g

Step 6) Multiply for the amount of mass employed in the adsorption point
26.14 mg BaP/g · 0.005 g = 0.1307 mgBaP/ S_{BET} · 7.5 mg

*This value represents the experimental surface coverage of BaP by 7.5 mg of CB Printex 90.

C) Final step

Step 7) To compute the percent coverage by of the CB Printex 90, we will employ the following equation:

% surface coverage = (Experimental coverage / theoretical value) × 100
% surface coverage = (0.131 / 0.184) × 100 = 70.7 %, suggesting the formation of a monolayer.